ISSN 0036-0244, Russian Journal of Physical Chemistry A, 2021, Vol. 95, Suppl. 1, pp. S140–S148. © Pleiades Publishing, Ltd., 2021.

STRUCTURE OF MATTER AND QUANTUM CHEMISTRY

Prediction of Joule–Thomson and Deviation Functions of Refrigerants at Low Pressure Using the Correlation Function

Mohsen Najafi[a,*]

[a] *Materials and Nuclear Fuel Research School, Nuclear Science and Technology Research Institute, AEOI, Tehran, Iran*

**e-mail: mnajafi@aeoi.org.ir*

Received June 14, 2020; revised August 4, 2020; accepted September 9, 2020

Abstract—In this paper, we calculate Joule–Thomson, the enthalpy changes relative to the pressure and deviation functions at low pressure for refrigerant fluids in order to evaluate the performance of their correlation function. The studied refrigerants are R11, R123, R124, R134a, R143a, R152a, R141b, R142b, R227ea, and R236ea. The studied corresponding state principle is the one suggested by Meng et al. In addition, to compare with the data obtained by others, Boyle temperature, Boyle volume, and maximum inversion temperature were also calculated using the correlation. The obtained results show that the correlation equation presented has a good ability to predict the thermophysical properties of materials and their deviation from the ideal state over a wide range of temperatures.

Keywords: correlation function, virial coefficients, refrigerants, Joule–Thomson coefficient, deviation function, maximum inversion temperature

DOI: 10.1134/S0036024421140168

INTRODUCTION

Refrigeration is a process of cooling or freezing a substance to a temperature lower than that of its surroundings and maintaining the substance in a cold state. Refrigeration can be accomplished by arranging heat transfer from a warm body through processes such as convection or thermal conduction. Refrigerant is a material used in the refrigeration process so that it vaporizes and cools as it passes through the throttling valve. The two main uses of refrigerants are refrigerators/freezers and air conditioners. Refrigerants must have suitable thermodynamic properties, and must be non-corrosive to mechanical components, non-toxic and non-flammable. In particular, refrigerants should not deplete the ozone layer and change the climate. For these reasons, some refrigerants that were previously widely used are now very limited in use such as chlorofluorocarbons (CFCs).

Given the importance of refrigerants, much research has been done to determine the physicochemical properties and their effects on the environment so far [1–6]. Over the past three decades, various studies have been conducted on substances that can be used as refrigerants while not destroying the ozone layer. The result of this research has been the introduction of refrigerants as a replacement for previous ones. Nowadays, lots of research are in the field of electrocaloric and elastocaloric refrigeration. Many of these technologies show the potential for progress in energy efficiency, compression, noise levels and environmental impacts [7].

In this paper, we calculate Joule–Thomson, the enthalpy changes relative to the pressure and deviation functions at low pressure for refrigerants fluids using their virial coefficients based on corresponding state principle.

Virial Coefficients

One of the important tools for the correlation and prediction of the thermodynamic properties of gases, liquids, and even solids over a wide range of temperatures and pressures is equation of state (EOS). Since they are a powerful tool for determining the data required, many publications deal with their development or improvement [8–10]. One of the oldest models for calculating the thermophysical properties of fluids is the virial equation of state (VEOS), which provides the required information with relatively good accuracy

$$Z = 1 + \sum_{n=2} B_n \rho^{n-1} \tag{1}$$

or

$$Z = 1 + \sum B_n^+ P^{n-1},$$
$$B_2^+ = B_2/RT, \tag{2}$$
$$B_3^+ = (B_3 - B_2^2)/R^2T^2,$$

where Z is the compressibility factor ($Z = pV_m/RT$), ρ is the density ($\rho = 1/V_m$), and B_n is nth virial coefficient. It is clear that when the pressure or density becomes zero, the compressibility factor will be one, and this is the ideal gas equation, $Z = 1$. Therefore, the virial equation shows the deviation from the ideal state. What is fundamentally important about VEOS is that it has a strong theoretical basis in statistical mechanics. In fact, The virial coefficients are related to intermolecular interactions by exact statistical-mechanical formulae. In this respect, nth virial coefficient are related to molecular interactions in clusters of n molecules. For example, the second coefficient indicates the interaction between the pair of molecules and, as the same way, the third coefficient to the interaction of the three molecules in the cluster, and so on. Thus, the virial coefficients are the connection bridge between microscopic and macroscopic properties and show the non-ideal behavior of real fluids [11]. From this view point, by accurately identifying the virial coefficients and how they depend on temperature and using VEOS, it can be easily to calculate the thermodynamic properties of fluids.

Virial coefficients can be obtained using both experimental and theoretical methods [11–23]. Experimental methods consist of *PVT* measurements, speed of sound measurements, Joule–Thomson measurements, refractive index and relative permittivity measurements and vapor pressure and enthalpy of vaporization measurements. Theoretical approaches usually consist of using equations of state and interaction potential functions.

Most of the research on virial coefficients is related to the second and third coefficients, and attempts are made to obtain a general correlation relationship for many molecules. In 1957, for the second virial coefficients of nonpolar gases, Pitzer and Curl [24] presented a successful correlation. Then this correlation has been modified by O'Connell and Prausnitz [25], Tsonopoulos [26, 27], Tarakad and Danner [28], Orbey [29], Weber [30], and Hayden and O'Connell [22] using refitting the coefficients of the Pitzer–Curl correlation, added polar and hydrogen bonding terms, applied new parameters, and so on.

For the third virial coefficients, in 1951, Rowlinson [31] calculated the third virial coefficients of polar molecules from the Stockmayer potential. In 1983, Orbey and Vera [32] provided an effective correlation for nonpolar gases. Van Nhu et al. [33] gave a correlation which was linked to the second virial coefficients with additional knowledge of the virial coefficients of hard convex body molecule. Weber [30] presented a successful correlation for polar haloalkanes adapting the model of Van Nhu et al. [33].

Among the substances whose virial coefficients have been studied so far, the virial coefficients of refrigerants have also been investigated due to their widespread industrial use [26, 27, 30, 32, 34–43]. In this research, we use the Meng's correlation for the second virial coefficient of fluids [44]. Meng developed the well-known Tsonopoulos correlation [26, 27] for second virial coefficients based on the corresponding-states principle for nonpolar gases, polar haloalkanes and other nonhydrogen bonding polar gases. The correlated and developed equation as follows

$$B_r = \frac{BP_c}{RT_c} = f^{(0)}(T_r) + \omega f^{(1)}(T_r) + f^{(2)}(T_r),$$
$$f^{(0)} = 0.1445 - \frac{0.330}{T_r} - \frac{0.1385}{T_r^2} - \frac{0.0121}{T_r^3} - \frac{0.000607}{T_r^8}, \quad (3)$$
$$f^{(1)} = 0.0637 + \frac{0.331}{T_r^2} - \frac{0.423}{T_r^3} - \frac{0.008}{T_r^8},$$
$$f^{(2)} = \frac{a}{T_r^6},$$

in which T_r ($=T/T_c$) is the reduced temperature, P_c and T_c are the critical pressure and critical temperature respectively, ω is the acentric factor and a is proposed to be function of the reduced dipole moment μ_r. Table 1 gives their critical properties and other parameters of studied refrigerants.

Joule–Thomson and Deviation Functions

In thermodynamics, the Joule–Thomson (J–T) effect is related to temperature change of a fluid when that fluid is forced to pass through a valve or porous plug so that heat is not exchanged with the environment. The J–T effect is of considerable importance in refrigeration and gas liquefaction processes. In this regard, the J–T coefficient (μ_{JT}) is defined as follows

$$\mu_{JT} = \left(\frac{\partial T}{\partial P}\right)_H. \quad (4)$$

This coefficient can be positive, negative or zero. In the range where the J–T coefficient is positive, the fluid cools by decreasing the fluid pressure. And if it is negative, as the pressure decreases, the temperature of the fluid increases. For refrigeration to occur, the thermodynamic state of the fluid must be in the area bounded by the inversion curve or the location of points where the J–T coefficient is zero ($\mu_{JT} = 0$). The inversion curve is plotted at T–P coordinates and is specific to each refrigerant. The range of this curve is from the minimum inversion temperature (T_{min}) for saturated state on the vapor pressure line to the maximum inversion temperature (T_{max}) for the ideal gas limit at zero density and pressure. Based on thermodynamic relations, we have

$$\mu_{JT} = -\frac{1}{C_{p,m}}\left(\frac{\partial H}{\partial P}\right)_T, \quad (5)$$

Table 1. Critical properties and other parameters of refrigerants [44, 45]

Refrigerant	Formula	T_c, K	P_c, atm	ρ_c, mol/L	N	ω	μ_r	a
R11	$CFCl_3$	471.110	43.50001	4.032963	5	0.18875	3.97	0.00614
R123	$CHCl_2CF_3$	456.831	36.1390	3.596418	8	0.28192	31.84	–0.00091
R124	$CHClFCF_3$	395.425	35.76901	4.103316	8	0.28810	49.36	–0.00069
R134a	CF_3CFH_2	374.210	40.0620	5.017053	8	0.32684	121.17	–0.00740
R143a	CF_3CH_3	345.857	37.1180	5.128450	8	0.2615	169.91	–0.01703
R152a	CHF_2CH_3	386.411	44.5769	5.571450	8	0.27521	152.76	–0.01661
R141b	$CFCl_2CH_3$	477.5	41.5690	3.921	8	0.22	77.50	–0.00132
R142b	$CClF_2CH_3$	410.26	40.020	4.438	8	0.232	109.29	–0.00452
R227ea	CF_3CHFCF_3	375.95	29.598	3.41	11	0.354	43.85	0.00245
R236ea	$CF_3CHFCHF_2$	412.44	34.5619	3.70302	11	0.3794	25.90	–0.00078

in which $C_{P,m}$ is heat capacity. As told before, thermodynamic properties of fluids can be easily calculated from a knowledge of the virial coefficients. In this sense, it can be shown that

$$\left(\frac{\partial H}{\partial P}\right)_T = -RT^2\left[\frac{dB^+}{dT} + \frac{dC^+}{dT}P + \frac{dD^+}{dT}P^2 + ...\right]. \quad (6)$$

According to Eqs. (5) and (6), the Joule–Thomson coefficient can be obtained by virial coefficients

$$\mu_{JT} = \frac{RT^2}{C_{P,m}}\left(\frac{dB^+}{dT} + \frac{dC^+}{dT}P + \frac{dD^+}{dT}P^2 + ...\right). \quad (7)$$

At last, Joule–Thomson coefficient can be shown as the expansion by pressure in which expansion coefficients depend on virial coefficients as follows

$$\mu_{JT} = \frac{1}{C_{P,m}}\sum_{n=0} A_n P^n = \frac{1}{C_{P,m}}(A_0 + A_1 P + ...),$$

$$A_0 = T\frac{dB}{dT} - B, \quad (8)$$

$$A_1 = \frac{1}{R}\left(\frac{dC}{dT} - 2B\frac{dB}{dT}\right) + \frac{2}{RT}(B^2 - C).$$

At zero pressure, we have

$$\mu^0_{JT}(T) = \frac{A_0(T)}{C^0_{P,m}} = \frac{1}{C^0_{P,m}}\left(T\frac{dB(T)}{dT} - B(T)\right), \quad (9)$$

in where μ^0_{JT} is Joule–Thomson coefficient at zero pressure. $C^0_{P,m}$ is the isobaric heat capacity of a molecule at zero pressure, or in other words, at ideal conditions. In this condition, we know

$$C^0_{P,m} = C^0_{V,m} + R, \quad (10)$$

$C^0_{V,m}$ is the isochoric heat capacity of a molecule at ideal conditions. Based on statistical thermodynamics and in a useful approximation, isochoric heat capacity includes the contributions of translational, rotational, and vibrational motions to the heat capacity as follows

$$C^0_{V,m} = C^0_{V,m,\text{trans}} + C^0_{V,m,\text{vib}} + C^0_{V,m,\text{rot}}. \quad (11)$$

Given the principle of equipartition of energy, each degree of freedom will contribute $RT/2$ to the energy and $R/2$ to the isochoric heat capacity at ideal conditions. This principle is exact for translational and rotational motions, then

$$C^0_{V,m,\text{trans}} = \frac{3}{2}R \quad \text{(3 degrees of freedom for all molecules)},$$
$$C^0_{V,m,\text{rot}} = \frac{3}{2}R \quad \text{(3 degrees of freedom for non-linear molecules)}. \quad (12)$$

For vibrational motions of non-linear molecules, we have

$$C^0_{V,m,\text{vib}} = \sum_{j=1}^{3N-6} C^0_{V,m,\text{vib},j} \quad \text{((3}N - 6\text{) degrees of freedom for non-linear molecules)}, \quad (13)$$

$$C^0_{V,m,\text{vib},j} = R\left(\frac{\theta_{\text{v}j}}{T}\right)^2 \frac{e^{\theta_{\text{v}j}/T}}{(e^{\theta_{\text{v}j}/T} - 1)^2},$$

in which N is number of atoms in molecule and $\theta_{\text{v}j} = h\nu_j/k$ that is called the vibrational characteristic temperature of vibrational mode j. It can be shown that vibrational isochoric heat capacity of mode j ($C_{V,m,\text{vib},j}$) in temperature range of 250 to 600 K for the studied refrigerants in this work, which includes different types of bonds such as C–Cl and C–F, is almost between $0.05R$ to R. In this case, to simplify the calculations and in a suitable approximation, value of $C_{V,m,\text{vib},j}$ can be considered $(1/2)R$ for all vibrational modes.

Due to above mentioned issues, it can be told that each degree of freedom of translational, rotational and vibrational motions will contribute $R/2$ to the isochoric heat capacity of molecule at ideal conditions. Then $C^0_{P,m}$ in a useful approximation is

$$C^0_{P,m} = C^0_{V,m} + R \approx \left(1 + \frac{\sigma}{2}\right) R, \quad (14)$$

where σ is the number of degrees of freedom of a molecule. Each atom has three degrees of freedom and therefore, a molecule with N atoms has $3N$ degrees of freedom. So

$$C^0_{P,m} \approx \left(1 + \frac{3}{2} N\right) R. \quad (15)$$

At last, given Eqs. (9) and (15), zero pressure J–T coefficient can be written as follows

$$\mu^0_{JT}(T) = \frac{1}{\left(1 + \frac{3}{2}\ N\right) R}\left(T \frac{dB(T)}{dT} - B(T)\right), \quad (16)$$

Joule–Thomson coefficient of ideal gas is zero, because there is no interaction between their molecules. However, Eqs. (9) and (16) show that J–T coefficient of real gas is not zero in the limit of zero pressure. In this regard, zero pressure J–T coefficient (μ^0_{JT}) can be used as a measure of the deviation from the ideal state due to the interactions related to the pair of molecules. These deviations can provide useful information about the nature of intermolecular forces.

Given Eqs. (5) and (8), the slope of the enthalpy changes relative to the pressure can be calculated

$$\left(\frac{\partial H}{\partial P}\right)_T = -\mu_{JT} C_{P,m} = -\sum_{n=0} A_n P^n = -(A_0 + A_1 P + ...) \quad (17)$$

and at zero pressure,

$$\left(\frac{\partial H}{\partial P}\right)^0_T = -\mu^0_{JT} C^0_{P,m} = -A_0, \quad (18)$$

where $\left(\frac{\partial H}{\partial P}\right)^0_T$ is the enthalpy changes relative to the pressure at ideal conditions. Also, as mentioned before in the inversion curve, maximum inversion temperature (T_{max}) corresponds to the ideal gas limit at zero density and pressure, then $\mu^0_{JT}(T_{max}) = 0$ or

$$A_0(T_{max}) = 0. \quad (19)$$

As told before, the virial coefficients are the connection bridge between microscopic and macroscopic properties and show the non-ideal behavior of real fluids. Therefore, having virial coefficients, non-ideality measurement can be calculated using deviation functions in different pressures and temperatures. Based on the thermodynamic relations for deviation function of enthalpy, we have

$$H^{id}_m(T,P) - H_m(T,P) = \int_0^P \left[T\left(\frac{\partial V_m}{\partial T}\right)_P - V_m\right] dP. \quad (20)$$

Deviation functions, the same as Joule–Thomson coefficient, can be written as the expansion by pressure in which expansion coefficients depend on virial coefficients as follows,

$$H^{id}_m(T,P) - H_m(T,P) = \sum_{n=1} b_n P^n,$$

$$b_1 = A_0 = T\frac{dB}{dT} - B, \quad (21)$$

$$b_2 = \frac{1}{2} A_1 = \frac{1}{2R}\left(\frac{dC}{dT} - 2B\frac{dB}{dT}\right) + \frac{1}{RT}(B^2 - C).$$

It is clear that deviation functions are equal to zero when $P = 0$ and of course, at low pressure, second terms onwards can be ignored in the expansion.

In our work, we calculate Joule–Thomson and deviation function of enthalpy at low pressure for refrigerant fluids using their virial coefficients based on corresponding state principle.

RESULTS AND DISCUSSION

In this paper, we chose 10 refrigerants R11, R123, R124, R134a, R143a, R152a, R141b, R142b, R227ea, and R236ea in order to determine their Joule–Thomson and deviation functions in low pressure. Figures 1–4 show the calculated zero pressure Joule–Thomson coefficient of some refrigerants versus temperature using the corresponding state principle. The obtained results are compared with experimental data from NIST [45]. As seen, with decreasing temperature, especially temperatures below the critical temperature, μ^0_{JT} increases sharply, and with increasing temperature, this coefficient goes to zero. This fluid behavior is, both qualitatively and quantitatively, predicted very well by the correlated equation in wide range of temperature. However, at low temperatures, especially in the ambient temperature range, deviations from experimental data can be seen. This deviation is more pronounced in the case of R11. It seems that the greater deviation in R11 is probably due to the fact that, firstly the correlation equation obtained for this material is not accurate enough at low temperatures. Second, the approximation used for vibrational isochoric heat capacity of mode j, $C_{V,m,vib,j} = (1/2)R$, does not seem appropriate for this material at low temperatures.

Figures 5 and 6 show the slope of enthalpy changes relative to pressure at different temperatures. The results are compared with experimental data. Experimental data were obtained from information about J–T coefficient and isochoric heat capacity of refrigerants available in NIST [45]. As seen, fluid behavior is, both qualitatively and quantitatively, predicted very

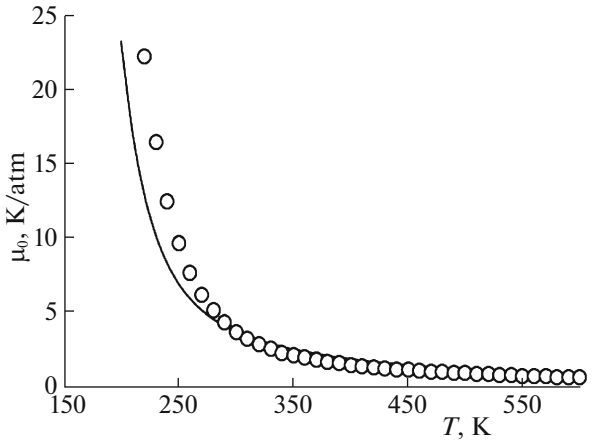

Fig. 1. Zero pressure Joule–Thomson coefficient of R11 versus temperature; line–this work; points–experimental data.

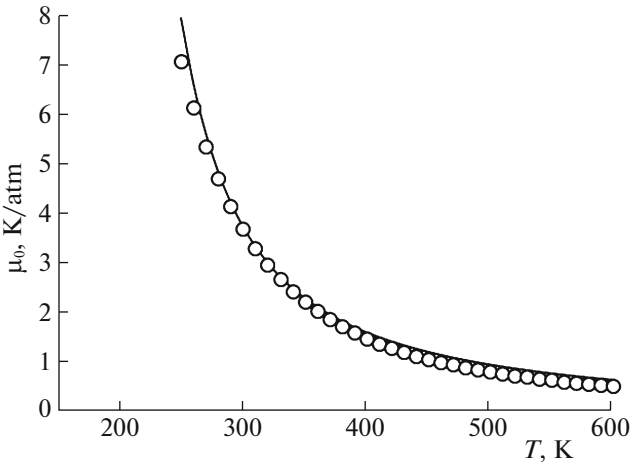

Fig. 2. Zero pressure Joule–Thomson coefficient of R123 versus temperature; line–this work; points–experimental data.

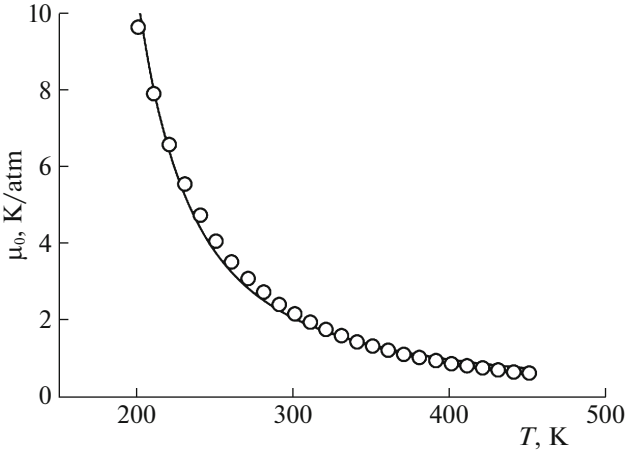

Fig. 3. Zero pressure Joule–Thomson coefficient of R124 versus temperature; line–this work; points–experimental data.

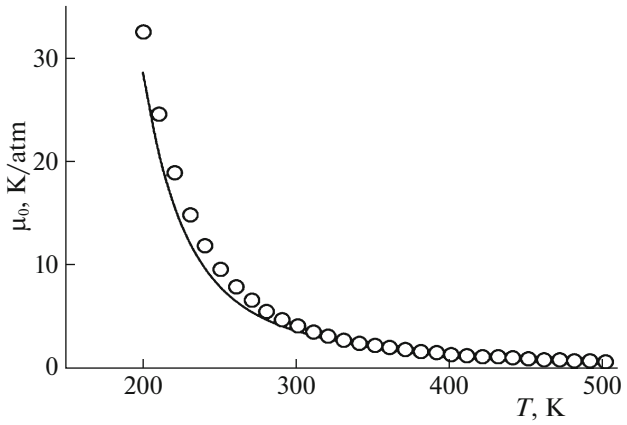

Fig. 4. Zero pressure Joule–Thomson coefficient of R141b versus temperature; line–this work; points–experimental data.

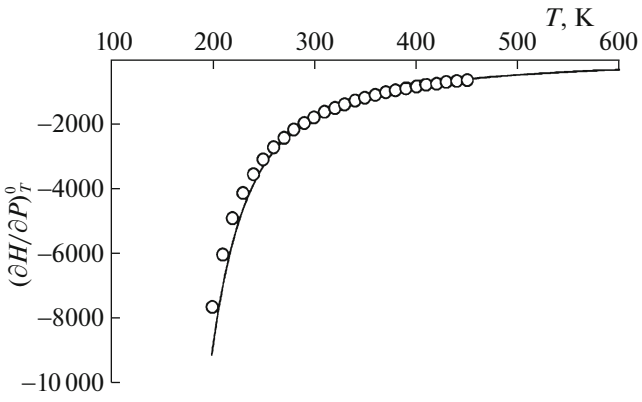

Fig. 5. The slope of enthalpy changes relative to pressure of R134a versus temperature; line–this work; points–experimental data.

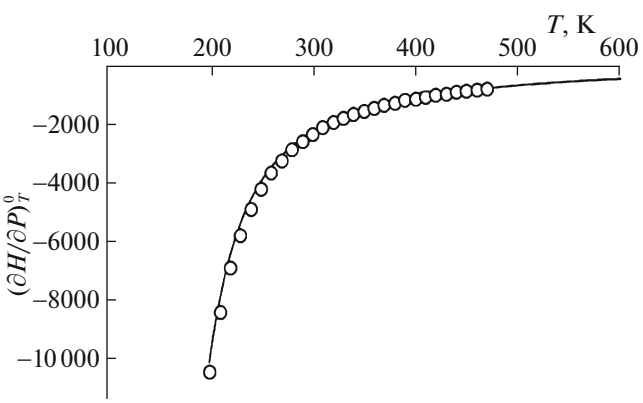

Fig. 6. The slope of enthalpy changes relative to pressure of R227ea versus temperature; line–this work; points–experimental data.

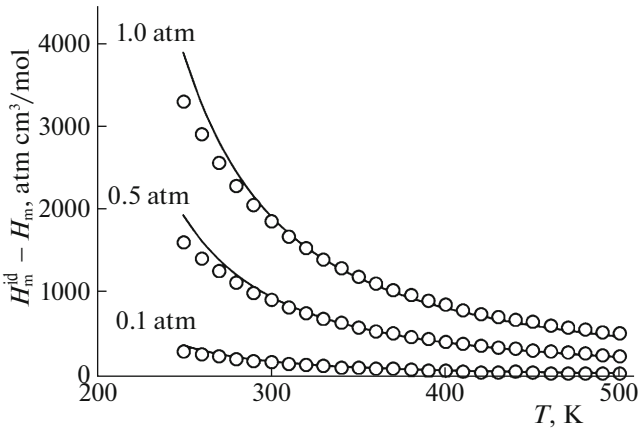

Fig. 7. Deviation function of enthalpy for R152a in different pressures; lines–this work; points–experimental data.

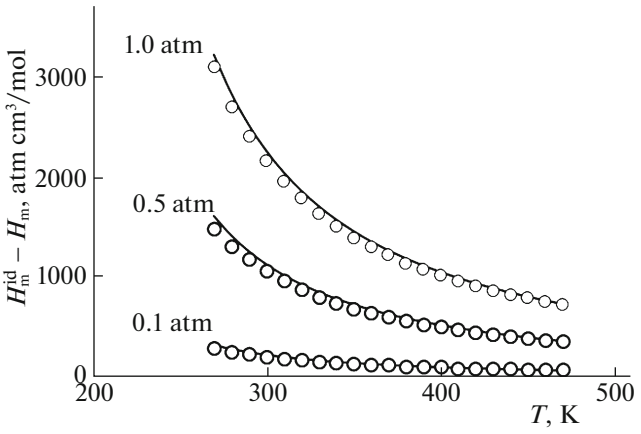

Fig. 8. Deviation function of enthalpy for R142b in different pressures; lines–this work; points–experimental data.

Table 2. Numerical values of changes μ_{JT}^0 and $(\partial H/\partial P)_T^0$ of R227ea with respect to temperature

T, K	μ_{JT}^0		$(\partial H/\partial P)_T^0$	
	exp.	calc.	exp.	calc.
200	10.239	7.008	−10385.9	−10064.0
210	7.946	5.548	−8367.6	−7966.8
220	6.301	4.506	−6871.0	−6470.6
230	5.095	3.748	−5740.0	−5383.0
240	4.192	3.182	−4868.7	−4569.7
250	3.503	2.747	−4187.2	−3945.5
260	2.970	2.406	−3645.4	−3455.2
270	2.549	2.132	−3208.3	−3061.9
280	2.213	1.908	−2851.8	−2740.5
290	1.940	1.722	−2556.7	−2473.5
300	1.717	1.565	−2310.0	−2248.6
310	1.531	1.432	−2101.6	−2056.7
320	1.376	1.317	−1923.8	−1891.1
330	1.244	1.216	−1770.7	−1746.9
340	1.131	1.128	−1637.9	−1620.3
350	1.034	1.050	−1521.7	−1508.2
360	0.950	0.981	−1419.3	−1408.4
370	0.876	0.918	−1328.4	−1318.9
380	0.811	0.862	−1247.3	−1238.4
390	0.754	0.811	−1174.6	−1165.5
400	0.703	0.765	−1108.8	−1099.2
410	0.657	0.723	−1049.3	−1038.7
420	0.616	0.685	−994.9	−983.4
430	0.579	0.649	−945.4	−932.5
440	0.545	0.617	−899.7	−885.7
450	0.514	0.587	−857.7	−842.4
460	0.486	0.559	−818.7	−802.3
470	0.460	0.533	−782.6	−765.0

well by the correlated equation in wide range of temperature. Table 2 shows numerical values of changes μ_{JT}^0 and $(\partial H/\partial P)_T^0$ of R227ea with respect to temperature in order to compare better between calculated and experimental data.

Since the Boyle temperature (T_B) and Boyle volume (V_B) was found to be sensitive to equation in use [46], therefore we determined them using correlation equation. The Boyle temperature (T_B) is the temperature in which $B(T_B)$ has changed the sign

$$\begin{cases} B(T) > 0 & \text{for} \quad T > T_B \\ B(T) < 0 & \text{for} \quad T < T_B \\ B(T) = 0 & \text{for} \quad T = T_B. \end{cases} \tag{22}$$

At this temperature, any gas behaves like an ideal gas. The Boyle volume (V_B) can be obtained as follows

$$V_B = T_B \left(\frac{\partial B}{\partial T}\right)_{T=T_B}. \tag{23}$$

The results are shown in Table 3 and compared with theoretical results in the literatures [47, 48]. As seen, our results have a very good agreement with the ones obtained Estrada-Torres et al. [48] but are in much differences with Mamedov's results [47].

Figures 7–10 show the calculated deviation function of enthalpy for refrigerants versus temperature in different pressures 0.1, 0.5, and 1.0 atm and the results have been compared with experimental data from NIST [45]. As can be seen, there is a very good match between experimental and theoretical results. In this regard, average absolute deviation (AAD, %) as Eq. (20) were computed and the results are presented in Table 4. As is clear, there is little difference between theoretical and experimental results, and this shows a

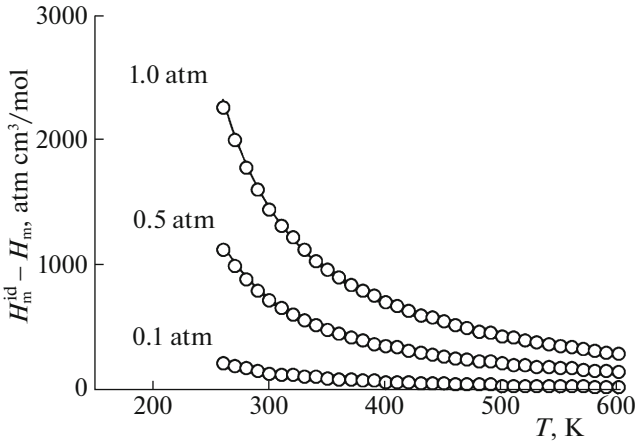

Fig. 9. Deviation function of enthalpy for R143a in different pressures; lines–this work; points–experimental data.

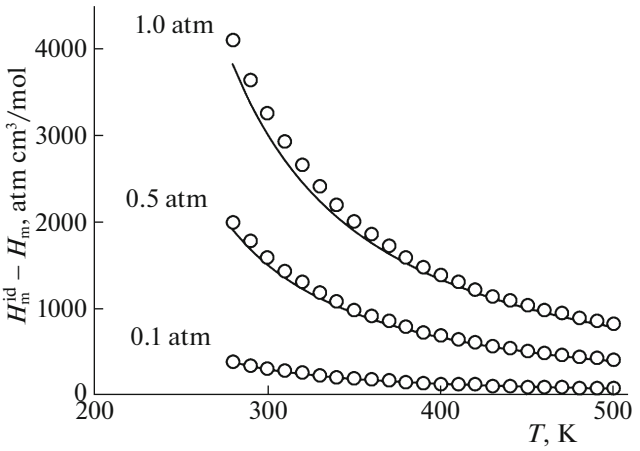

Fig. 10. Deviation function of enthalpy for R236ea in different pressures; lines–this work; points–experimental data.

good accuracy of the mentioned correlation in determining the thermophysical properties that can be calculated through the virial coefficients:

$$\text{AAD, \%} = \frac{1}{\text{NP}}\sum\left|\frac{(H_m^{\text{id}} - H_m)_{\text{exp}} - (H_m^{\text{id}} - H_m)_{\text{calc}}}{(H_m^{\text{id}} - H_m)_{\text{exp}}}\right| \times 100, \quad (24)$$

in which NP is the number of data points.

As told before, maximum inversion temperature (T_{max}) corresponds to the ideal gas limit at zero density and pressure where $\mu_{JT}^{0}(T_{\text{max}}) = 0$ or $A_0(T_{\text{max}}) = 0$ in the inversion curve. This temperature can be calculated using correlation equation and Table 3 shows the obtained T_{max} for above mentioned refrigerants. In this context, due to the lack of experimental results, it is not possible to compare the obtained data with the experimental data. However, due to the good compatibility of J–T coefficient and deviation function obtained with the experimental data, it seems that the obtained maximum inversion temperature T_{max} can be considered to some extent accurate.

CONCLUSION

In this paper, we calculated Joule–Thomson and deviation functions in low pressure for refrigerants fluids in order to evaluate the performance of their correlation equation in low pressure and wide range of temperature. For this purpose, 10 refrigerants of methane, ethane and propane derivatives were selected and studied. In addition, to compare with the data obtained by other authors, Boyle temperature, Boyle volume and maximum inversion temperature

Table 3. Calculated Boyle temperature (T_B), Boyle volume (V_B), and maximum inversion temperature (T_{max}) of refrigerants

Refrigerant	T_B			V_B	T_{max}
	this work	[47]	[48]		
R11	1135.5	959.367	1151.10	162.3083	2185
R123	1052.3	2933.57	1058.40	199.6492	2017
R124	908.5	2495.67	926.63	175.2652	1741
R134a	844.5	2356.15	875.33	151.5997	1614
R143a	805.2	1012.95	828.70	145.8740	1544
R152a	893.7	1012.12	938.69	136.7712	1713
R141b	1133.6	2138.96	1141.20	175.3004	2179
R142b	968.4	1327.26	982.17	157.5616	1860
R227ea	837.5	—	852.28	209.0922	1599
R236ea	908.3	—	923.03	199.5428	1732

Table 4. Temperature range and AAD, % in deviation function of studied refrigerants

Refrigerant	NP	T, K	AAD, %		
			$P = 0.1$	$P = 0.5$	$P = 1.0$
R11	31	300–600	3.65	3.97	4.76
R123	30	310–600	3.94	3.24	3.68
R124	21	270–470	2.83	1.08	0.63
R134a	21	250–450	3.13	1.77	1.57
R143a	38	230–600	5.75	3.58	3.43
R152a	26	250–500	5.91	5.43	4.87
R141b	20	310–500	5.50	4.95	4.17
R142b	21	270–470	6.18	4.55	3.30
R227ea	22	260–470	3.38	2.98	3.88
R236ea	23	280–500	5.25	4.47	5.23

were also calculated. A review of the figures, tables and results shows that the correlation equation presented has a good ability to predict the thermophysical properties of materials and their deviation from the ideal state over a wide range of temperatures.

Of course, for a more accurate conclusion, other thermodynamic functions that can be calculated using the virial coefficients. In this regard, the study of entropy deviation functions, determination of inversion curve in a wide range of temperature and pressure, determination of intermolecular potentials via inversion method, determination of Joule–Thomson coefficient in a wide range of temperature and pressure and etc., will be of importance. In this respect, other refrigerants and materials should be studied to evaluate correlation equations. The aforementioned studies will be our future research.

ACKNOWLEDGMENTS

The authors express their appreciations to Nuclear Science and Technology Research Institute (NSTRI) for supporting this work.

REFERENCES

1. C. H. de Paula, W. M. Duarte, T. T. M. Rocha, R. N. de Oliveira, and A. A. T. Maia, Int. J. Refrig. **113**, 10 (2020).
2. A. Mota-Babiloni, M. Mastani Joybari, J. Navarro-Esbri, C. Mateu-Royo, A. Barragán-Cervera, M. Amat-Albuixech, and F. Molés, Int. J. Refrig. **111**, 147 (2020).
3. A. Maiorino, C. Aprea, M. G. del Duca, R. Llopis, D. Sánchez, and R. Cabello, Int. J. Refrig. **96**, 106 (2018).
4. P. Dhankhar, Int. J. Sci. Res. **3**, 1212 (2014).
5. C. Kwang-Seop, K. Min Soo, K. Yongchan, and K. Cho, Korean J. Air-Condit. Refrig. Eng. **12**, 1234 (2004).
6. K. Nagalakshmi and G. Marurhiprasad Yadav, Int. J. Eng. Res. Appl. **4**, 638 (2014).
7. A. Kitanovski, U. Plaznik, U. Tomc, and A. Poredos, Int. J. Refrig. **57**, 288 (2015).
8. Y. S. Wei and R. J. Sadus, AIChE J. **46**, 169 (2000).
9. J. O. Valderrama, Ind. Eng. Chem. Res. **42**, 1603 (2003).
10. F. de J. Guevara-Rodriguez, Fluid Phase Equilib. **307**, 190 (2011).
11. M. J. Assael, J. P. M. Trusler, and T. F. Tsolakis, *An Introduction to their Prediction Thermophysical Properties of Fluids* (Imperial College Press, London, UK, 1996).
12. L. Meng and Y.-Y. Duan, Fluid Phase Equilib. **238**, 229 (2005).
13. R. M. Gibbons, Cryogenics **14**, 399 (1974).
14. J. J. Martin, Ind. Eng. Chem. Fundam. **23**, 454 (1984).
15. A. Vetere, Fluid Phase Equilib. **164**, 49 (1999).
16. M. Ramos-Estrada, G. A. Iglesias-Silva, K. R. Hall, and F. Kohler, Fluid Phase Equilib. **240**, 179 (2006).
17. A. H. Harvey and E. W. Lemmon, J. Phys. Chem. Ref. Data **33**, 369 (2004).
18. J. Tian, Y. Gui, and A. Mulero, J. Phys. Chem. B **114**, 13399 (2010).
19. H. W. Xiang, Chem. Eng. Sci. **57**, 1439 (2002).
20. E. Holleran, Fluid Phase Equilib. **251**, 29 (2007).
21. D. X. Liu and H. W. Xiang, Int. J. Thermophys. **24**, 1667 (2003).
22. J. G. Hayden and P. O. O'Connell, Ind. Eng. Chem. Process Des. **14**, 209 (1975).
23. A. Khoshsima and A. Hosseini, J. Mol. Liq. **242**, 625 (2017).
24. K. S. Pitzer and R. F. Curl, J. Am. Chem. Soc. **79**, 2369 (1957).
25. J. P. O'Connell and J. M. Prausnitz, Ind. Eng. Chem. Process. Des. Dev. **6**, 245 (1967).

26. C. Tsonopoulos, AIChE J. **20**, 263 (1974).
27. C. Tsonopoulos, AIChE J. **21**, 827 (1975).
28. R. R. Tarakad and R. P. Danner, AIChE J. **23**, 685 (1977).
29. H. A. Orbey, Chem. Eng. Commun. **65**, 1 (1988).
30. L. A. Weber, Int. J. Thermophys. **15**, 461 (1994).
31. J. S. Rowlinson, J. Chem. Phys. **19**, 827 (1951).
32. H. Orbey and J. H. Vera, AIChE J. **29**, 107 (1983).
33. N. Van Nhu, G. A. Iglesias-Silva, and F. Kohler, Ber. Bunsenges. Phys. Chem. **93**, 526 (1989).
34. L. A. Weber, J. Chem. Eng. Data **35**, 237 (1990).
35. L. A. Weber and D. R. Defibaugh, J. Chem. Eng. Data **41**, 1477 (1996).
36. S. J. Boyes and L. A. Weber, Int. J. Thermophys. **15**, 443 (1994).
37. B. Schramm and C. H. Weber, J. Chem. Thermodyn. **23**, 281 (1991).
38. A. R. H. Goodwin and M. R. Moldover, J. Chem. Phys. **95**, 5236 (1991).
39. A. Yokozeki, H. Sato, and K. Watanabe, Int. J. Thermophys. **19**, 89 (1998).
40. S. Nakamura, K. Fujiwara, and M. Noguchi, J. Chem. Eng. Data **42**, 334 (1997).
41. K. A. Gillis, Int. J. Thermophys. **18**, 73 (1997).
42. T. Tamatsu, T. Sato, H. Sato, and K. Watanabe, Int. J. Thermophys. **13**, 985 (1992).
43. G. di Nicola, G. Coccia, M. Pierantozzi, and M. Falone, Int. J. Refrig. **68**, 242 (2016).
44. L. Meng, Y.-Y. Duan, and L. Li, Fluid Phase Equilib. **226**, 109 (2004).
45. NIST Chemistry WebBook. www.nist.gov.
46. C. F. Leibovici and D. V. Nichita, Fluid Phase Equilib. **289**, 94 (2010).
47. B. A. Mamedov and E. Somuncu, J. Thermophys. Heat Transfer (2020, in press)
48. R. Estrada-Torres, G. A. Iglesias-Silva, M. Ramos-Estrada, and K. R. Hall, Fluid Phase Equilib. **258**, 148 (2007).